

**ESTIMATION OF CRITICAL DIMENSIONS  
FOR THE CRACK AND PITTING CORROSION  
DEFECTS IN THE OIL STORAGE TANK  
USING FINITE ELEMENT METHOD  
AND TAGUCHI APPROACH**

**MOSTAFA OMIDI-BIDGOLI<sup>1</sup>, KAZEM REZA-KASHYZADEH<sup>2</sup>  
and ALIREZA AMIRI-ASFARJANI<sup>3</sup>**

<sup>1</sup>Department of Mechanical Engineering  
Islamic Azad University  
Badroud Branch  
Badroud  
Iran  
e-mail: [mostafaomidibidgoli@gmail.com](mailto:mostafaomidibidgoli@gmail.com)

<sup>2</sup>Laboratory Head  
Mechanical Characteristics Lab  
Center for Lab Services  
Sharif University of Technology  
Tehran  
Iran  
e-mail: [Kazem.kashyzadeh@gmail.com](mailto:Kazem.kashyzadeh@gmail.com)  
[k\\_kashyzadeh@mehr.sharif.edu](mailto:k_kashyzadeh@mehr.sharif.edu)

<sup>3</sup>Department of Mechanical Engineering  
Qom University  
Qom  
Iran  
e-mail: [ar.amiri@qom.ac.ir](mailto:ar.amiri@qom.ac.ir)

---

Keywords and phrases: critical size, crack, pitting corrosion, oil storage tank, FEM, Taguchi approach.

Received November 21, 2018; Revised December 1, 2018; Accepted December 9, 2018

### **Abstract**

Oil storage tanks play an important role in storing crude oil. Therefore, proper care and its service are important for oil companies. In this regard, knowledge on the state of critical conditions of existing various defects, such as cracks and pitting corrosion defects, can play an essential role in providing a better service to these huge metal structures. In the present research, the basic theories are discussed for the crack defect. Then, an oil reserve in one of the island states of the country was modeled and was analyzed by considering different types of defects using finite element simulation. Then, critical dimensions of cracks and corrosion holes were identified in a number of cases. Eventually, the Taguchi approach was used to investigate the effect of different parameters related to the various defects such as length, depth and diameter on the maximum stress. The results indicated that the effect of crack and pitting corrosion depth is more than the effect of length and diameter for defects of crack and pitting corrosion, respectively.

### **1. Introduction**

Nowadays, reservoirs are widely used in various industries, especially the oil, gas and petrochemical companies. So that their exact and stable efficiency is important for storing different materials. In this case, crude oil storage tanks also need to be kept properly, which is important when it is possible to identify the situation and critical conditions of defects during the cyclic inspections.

Most important defects in these huge metal structures are crack and pitting corrosion. The first attempts to solve the cracked cylinder problem have been carried out by Underwood in 1972 [1]. Then, in 1982, Raju and Newman [2] have analyzed longitudinal cracks in pressure vessels using a 3-D finite element model. In 1993, Carpinteri [3] has utilized finite element simulation to analyze the semi-elliptical cracks in metal bars under uniaxial loading. After that Carpinteri et al. [4] have reported similar results for the behaviour of semi-elliptical cracks in tubes under cyclic flexural moment. Fonte et al. [5, 6] have examined a circular rod with an elliptical sidewall crack. In a participatory program in Canada, several experiments have been conducted to predict the failure behaviour of a damaged pressure vessel [7]. Then, Carpinteri et al. [8] has conducted research on the cracked tubes. Following these activities, a number of high-pressure cylinders of aluminum and steel have been

tested under hydrostatic pressure by the center of USA non-destructive testing analysis [9]. Shahani et al. [10, 11] have calculated the stress intensity factor for a semi-elliptical crack in the thick-walled cylindrical tank under bending moment using finite element analysis and experiment data. Recently, a new technique has been presented to predict the stress intensity factor of Mode I for an elliptical crack in the tube [12]. Moreover, stress intensity factor has been calculated for a semi-elliptical crack in the hollow cylinder tank under combined loadings [13]. Kaptan and Kisioglu [14] have performed some tests to determine the explosion pressure and critical region in the vehicle's gas cylinders. Also, laboratory investigations have been carried out on the critical region of the pressure vessels and compared with analytical results [14]. Kasai et al. [15] have evaluated back-side flaws of the bottom plates on the oil storage tank. Kim et al. [16] have carried out a failure analysis of fillet joint cracking in an oil storage tank. Godoy and Batista-Abreu [17] has obtained buckling of fixed-roof aboveground oil storage tanks under heat induced by an external fire. Yang et al. [18] have derived an analytical formula for elastic-plastic instability of large oil storage tanks. Kasai et al. [19] have predicted maximum depth of corrosion in an oil storage tank using extreme value analysis and Bayesian inference. Cheng et al. [20] have studied stability parameter analysis of a composite foundation of an oil storage tank in a loess area treated with compaction pile.

In this research, the most important defects in one of the reservoirs with a capacity of 1350000 barrels were investigated and analyzed. The critical size of cracks and pitting corrosion were determined. Taguchi approach and analysis for the various defects of corrosion has been applied for the first time. The results obtained by analyzing the defects and identifying critical dimensions can be useful in order to improve the inspection and prevention of future events.

## **2. Types of Defects in the Oil Storage Tanks**

The most important defects in the oil storage are crack and pitting corrosion. Generally, these defects are due to one of the following reasons:

(1) Defects due to inaccuracy in the construction, implementation, and assembling of the structure.

(2) Defects that occur during storage of oil and exploitation of reservoirs.

### 2.1. Pitting corrosion

Corrosion effects in oil storage tanks are divided into both internal and external types. Mostly corrosion occurs in the bottom of the oil storage tanks, which sometimes completely pierces the surface. The pit is a highly localized corrosion that also causes metal holes. These holes may have different diameters, but in most cases, their diameter is small. The pits are sometimes separated and sometimes close together to form a roughness surface. Pitting is one of the most destructive and worst types of corrosion. Because of the perforation of metals become unusable. However, the weight loss due to this corrosion is negligible [21]. Figure 1 shows the corrosion phenomenon at the bottom of an oil storage tank.

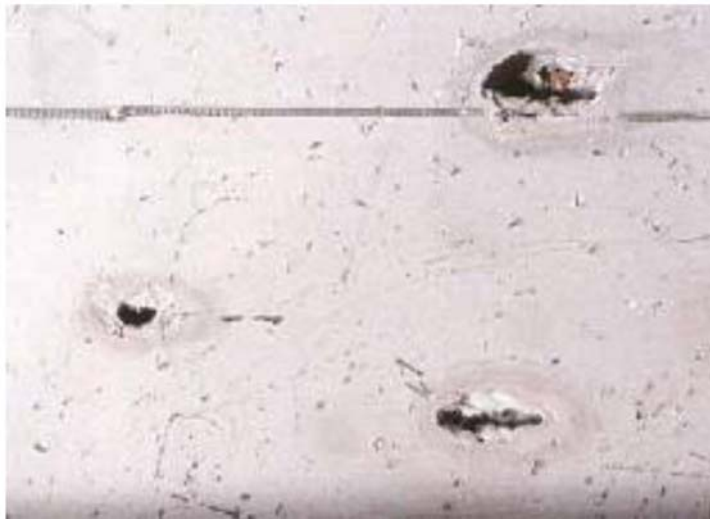


**Figure 1.** The defect of pitting corrosion at the bottom of an oil storage tank.

Corrosion researchers believe that the best coatings when used along with the cathodic protection system only reduce the corrosion rate of 70% and can never be reduced to zero. Although corrosion cannot be completely eliminated, its effects can be minimized by applying new methods such as cathodic protection, industrial coatings and so on.

## 2.2. Crack

Crack is one of the defects that rarely have been observed in oil storage tanks. However, the nature of these cracks is small, and is most commonly found in the weld areas. Certainly, these cracks will grow and can destroy the reservoir. In welding structures, a variety of arrangement is needed to prevent defects. Typically, the failure of pressure vessels during their service life will result in irreparable damage that not only causes economic losses. In the design of pressure vessels, attention should be paid to the issue of stress concentration on the inside of the weld, especially, containers that have been kept in service for a long time [22].

## 3. Finite Element Simulation

In the present study, the geometric characteristics of the oil storage tank are reported in Table 1 and the image of this tank is shown in Figure 2.

**Table 1.** Geometric characteristics of the oil storage tank

Parameter	Value	Unit
Diameter	119.5	Meter
Height	19	Meter
Type of roof	Floating	



**Figure 2.** Image of the oil storage tank which is studied in this research.

The oil storage tank is modeled in finite element software (ABAQUS) using element type of S4R as a shell body. The mesh convergence has been investigated and the final finite element model is prepared with the number of 30000 elements (Figure 3). The boundary conditions are considered as follow:

Around of tank floor:

$$u_1 = u_2 = u_3 = u_{R1} = u_{R2} = u_{R3} = 0. \quad (1)$$

The external surface of the tank floor:

$$u_3 = 0. \quad (2)$$

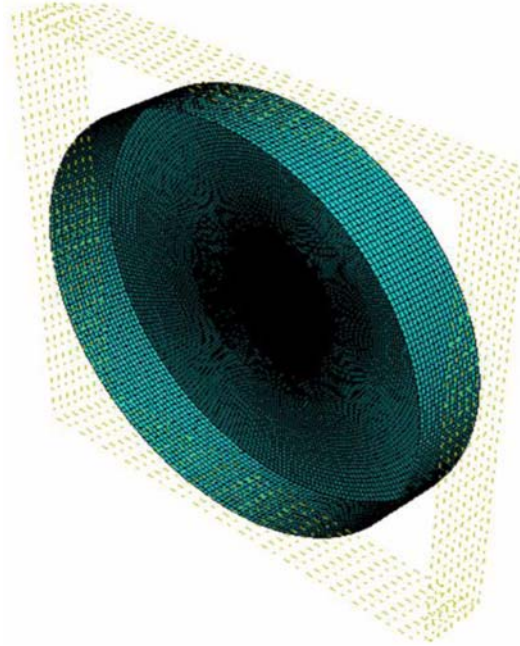


**Figure 3.** Finite element model of the oil tank.

The oil storage tank without any defects is analyzed under the hydrostatic pressure ( $p = \rho gh = 160295.4\text{Pa}$ ) in order to determine the critical region. After that, the defect behaviour is investigated and the critical stress is obtained using two different methods (analytical and FEM).

### 3.1. Analytical solution

Environmental and axial stresses in a cylinder are calculated in the following form [23]:

$$\sigma_h = \frac{P.R}{B}, \quad (3)$$

$$\sigma_a = \frac{P.R}{2B}, \quad (4)$$

where  $R$  and  $B$  are radius and thickness of tank, respectively. The tank wall is made up 8 different thickness sections with a constant height of 375mm. eventually, the maximum stress has been obtained equal to 222.7MPa.

### 3.2. FE solution

The maximum critical stress has been obtained using ABAQUS software. This value is 218.7MPa which has a good accuracy in compared with the analytical result (1.79% error). The contour of equivalent Von Misses stress is illustrated in Figure 4.

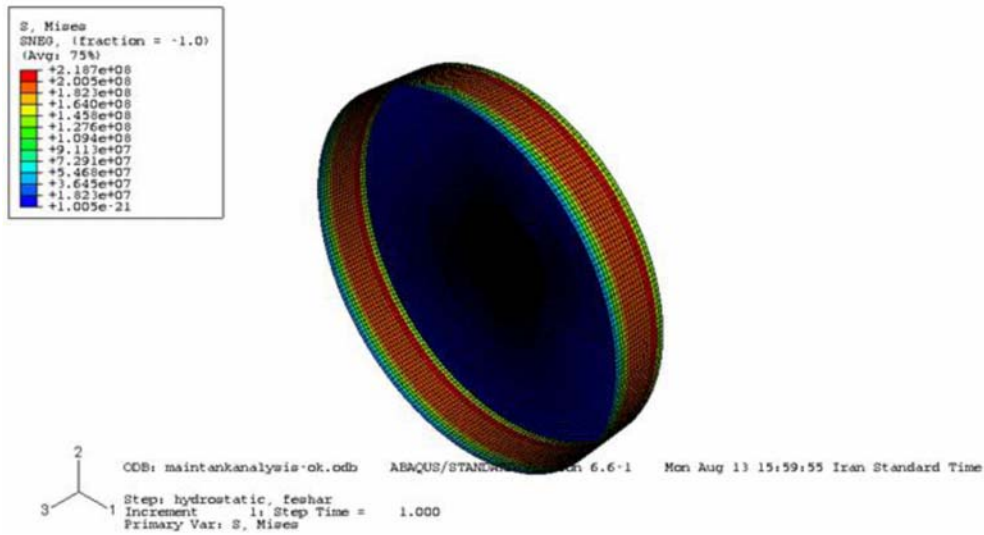


**Figure 4.** Von Misses stress contour of oil storage tank under the hydrostatic pressure.

### 3.3. Finite element model of crack and pitting corrosion

There are various techniques to model crack and corrosion defects using FEM. One of these methods is the shell to solid coupling elements in which multi-point constraints are used as demonstrated in Figure 5. In fact, the FE software provides continuity and integrity between the shell and solid elements by assigning special constraints [24, 25].



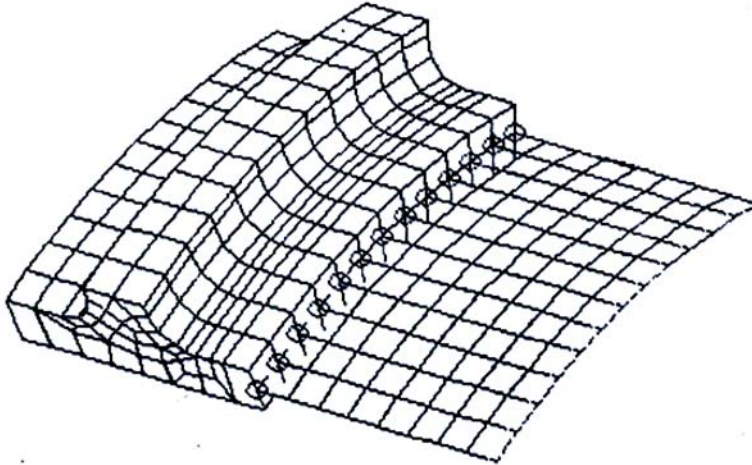


**Figure 5.** Schematic of the shell to solid coupling elements.

Firstly, a complete model was modeled using shell elements to validate this technique. Then, a new model with the same conditions was analyzed by utilizing a combination of shell and solid elements. In this regard, a middle part of the shell was modeled as the volume. The contour of Von Misses stress for both models are illustrated in Figure 6.

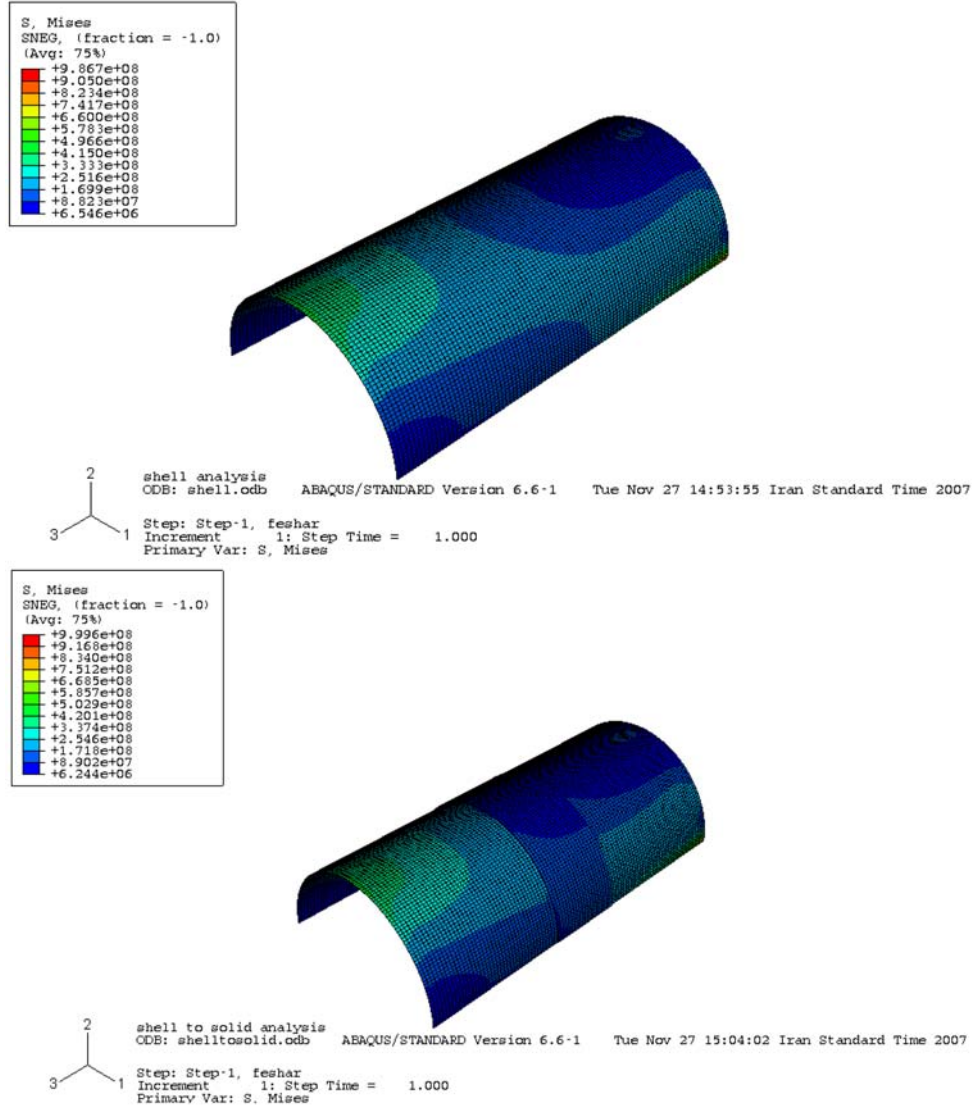


**Figure 6.** The contour of equivalent Von Mises stress for both FE models: (a) completely shell element and (b) combination of shell and solid elements.

As shown in Figure 6, the difference between the results of various models (von Misses stress) is about 1.3%. Also, the deformation is equal in each model. Therefore, this method can be used with a good accuracy for modeling and analyzing defects.

#### 4. Taguchi Approach

Taguchi method [26-31] has been used to determine the effect of different parameters of various defects including crack and pitting corrosion on the critical equivalent stress of oil storage tank. In this research, two different TM (Taguchi Algorithm) was designed with a mixed number of variables and levels to study the effects of various defects. Firstly, one parameter with 4 levels and other with 2 levels were considered for crack defects in different angles as reported in Table 2. The variable parameters considered in Taguchi algorithm with their different levels for pitting corrosion defect are reported in Table 3.

**Table 3.** Characteristics of variable parameters considered in the Taguchi algorithm for pitting corrosion defect

Levels	Variables	
	Parameter I: Depth	Parameter II: Length
A	50	10
B	100	15
C	150	20

The Taguchi orthogonal matrix with the characteristic  $L8(4^1 \& 2^1)$  and  $L9(3^2)$  are used to form the Taguchi analysis for defects of crack and pitting corrosion as shown in Table 4 and Table 5, respectively.

**Table 4.** The layout of orthogonal matrix L8 (stress is in MPa)

Angle	Run No.	Inputs		Output
		Parameter I	Parameter II	Stress
Zero	1	A	A	415.00
	2	A	B	415.20
	3	B	A	416.96
	4	B	B	417.60
	5	C	A	417.20
	6	C	B	418.00
	7	D	A	418.50
	8	D	B	419.00
45	1	A	A	416.40
	2	A	B	416.58
	3	B	A	417.40
	4	B	B	417.80
	5	C	A	418.20
	6	C	B	418.40
	7	D	A	419.00
	8	D	B	419.20
90	1	A	A	409.00
	2	A	B	409.11
	3	B	A	410.97
	4	B	B	412.35
	5	C	A	411.78
	6	C	B	412.42
	7	D	A	417.10
	8	D	B	417.73

**Table 5.** The layout of orthogonal matrix L9 (stress is in MPa)

Run No.	Inputs		Output
	Parameter I	Parameter II	Stress
1	A	A	415.13
2	A	B	417.41
3	A	C	419.63
4	B	A	415.61
5	B	B	419.70
6	B	C	421.83
7	C	A	416.44
8	C	B	418.55
9	C	C	436.9

## 5. Results and Discussion

### 5.1. Finite element results

To determine the critical sizes of oil storage tanks' defects, cracks and pits with different lengths, diameters, and depths are analyzed. Critical states have been identified by selecting the stress field close to the yield stress of the target area (416.66MPa). Surface defects are modelled by using C3D8R elements in the critical region. The stress diagrams are depicted in terms of depth for crack and pitting corrosion in various situations (Figure 7 and Figure 8).

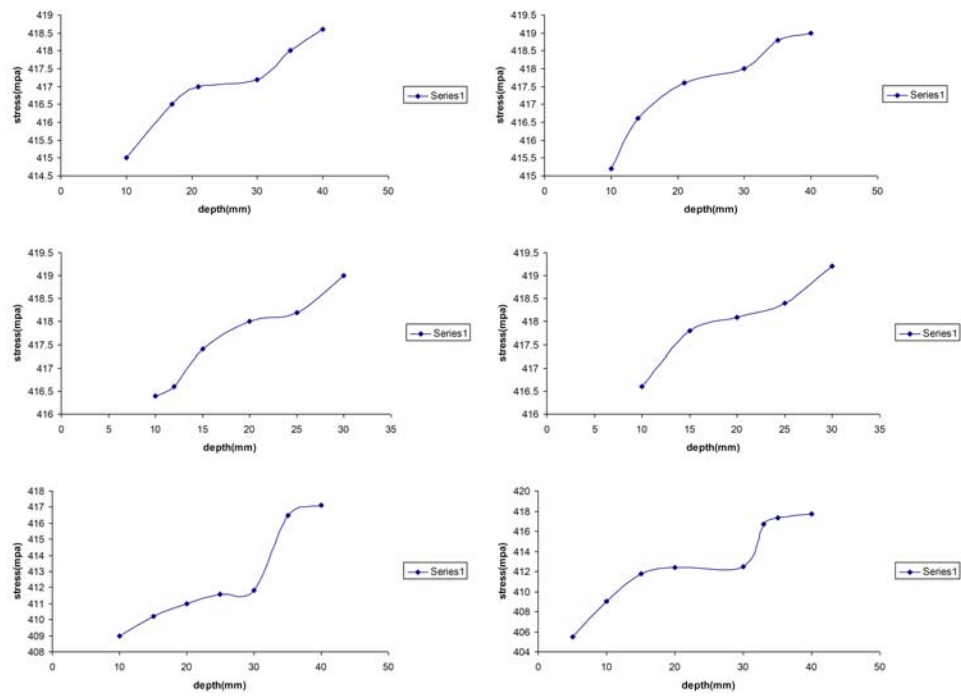


**Figure 7.** The stress diagram in terms of depth for crack in various length and angle: (a) length = 300 and angle = 0; (b) length = 400 and angle = 0; (c) length = 150 and angle = 45; (d) length = 200 and angle = 45; (e) length = 300 and angle 90; and (f) length = 400 and angle = 90.

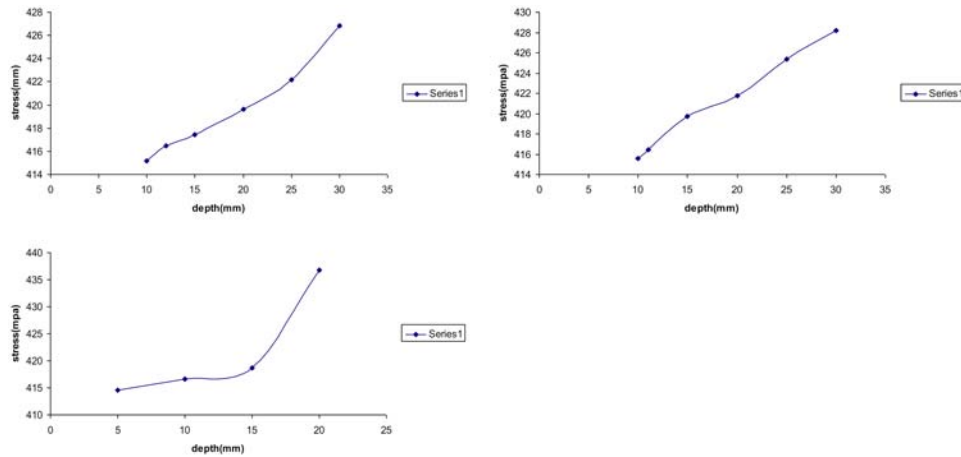


**Figure 8.** The stress diagram in terms of depth for pitting corrosion in various diameter: (a) diameter = 50mm; (b) diameter = 100mm; and (c) diameter = 150mm.

According to the results obtained from finite element analysis, the critical dimensions of the crack and the pitting corrosion defect are reported in Tables 2 and 3, respectively.

**Table 2.** The critical sizes for crack defect

Crack type	Critical dimensions		
	Length (mm)	Depth (mm)	Angle
Environmental crack	300	17	0
Environmental crack	400	14	0
Crack	150	12	45
Crack	200	10	45
Longitudinal crack	300	35	90
Longitudinal crack	400	33	90

**Table 3.** The critical sizes for pitting corrosion defect

Defect type	Critical sizes	
	Diameter (mm)	Depth (mm)
Corrosion cavity	50	12
Corrosion cavity	100	11
Corrosion cavity	150	10

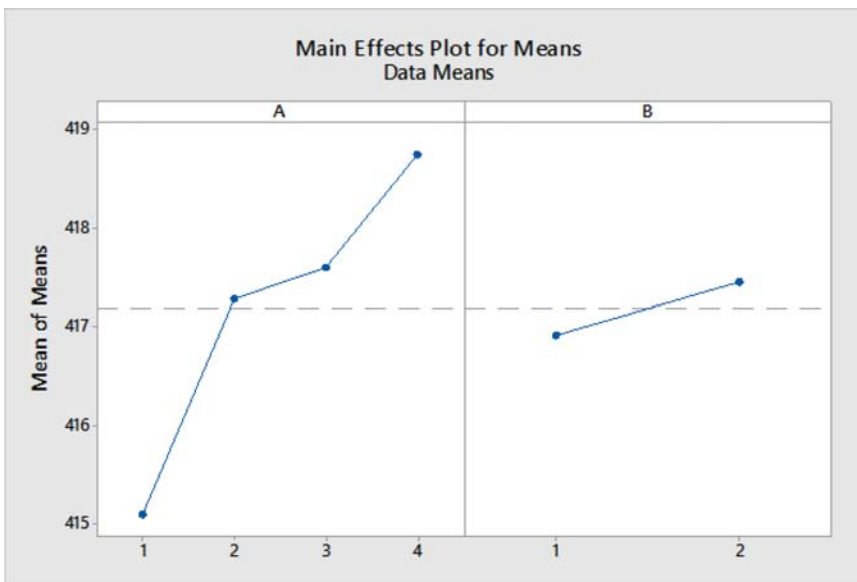
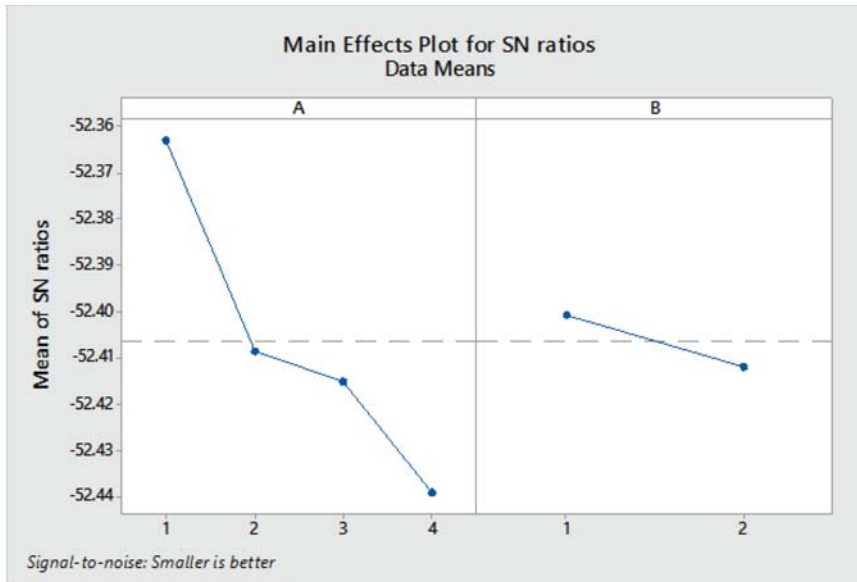
## 5.2. Taguchi results

The most effective and least effective parameter based on Taguchi's analysis, along with the percentage of each parameter, is determined. Given the need to reduce the equivalent Von Misses stress at the critical region of the oil storage tank, a smaller term is best used for data analysis in accordance with the following formula:

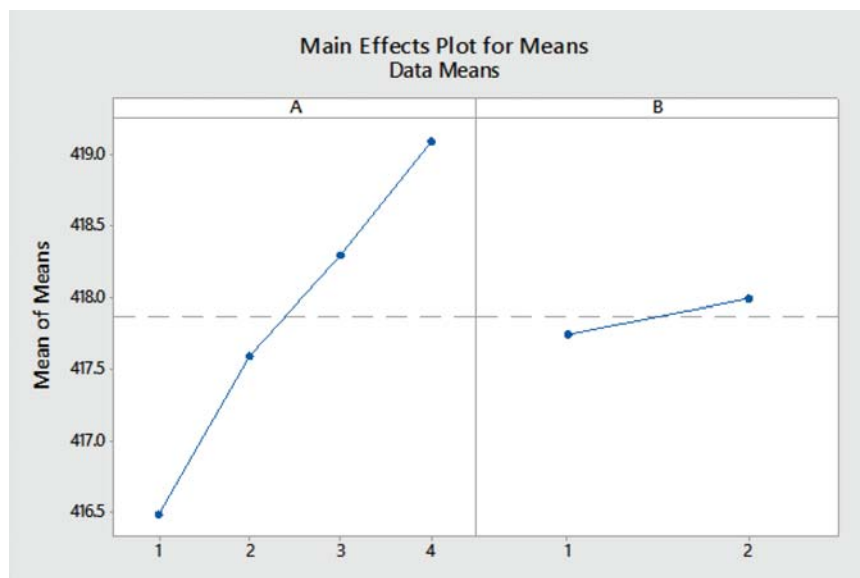
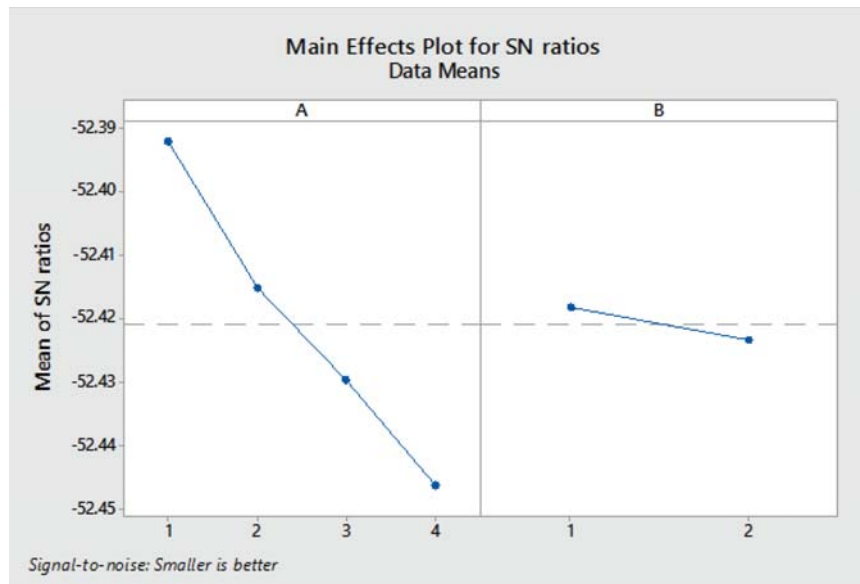
$$S/N = -10\text{Log}\left[\frac{1}{n}(y_1^2 + y_2^2 + \dots + y_n^2)\right], \quad (5)$$

where  $y_1, y_2, \dots, y_n$  represent the measured bent angles in the bending process, and each bending condition is repeated  $n$  times. Afterwards, the main influences of S/N ratios and mean ratios at every parameter level were analyzed and plotted in Figure 9 and Figure 10 for defects of crack and pitting corrosion, respectively.

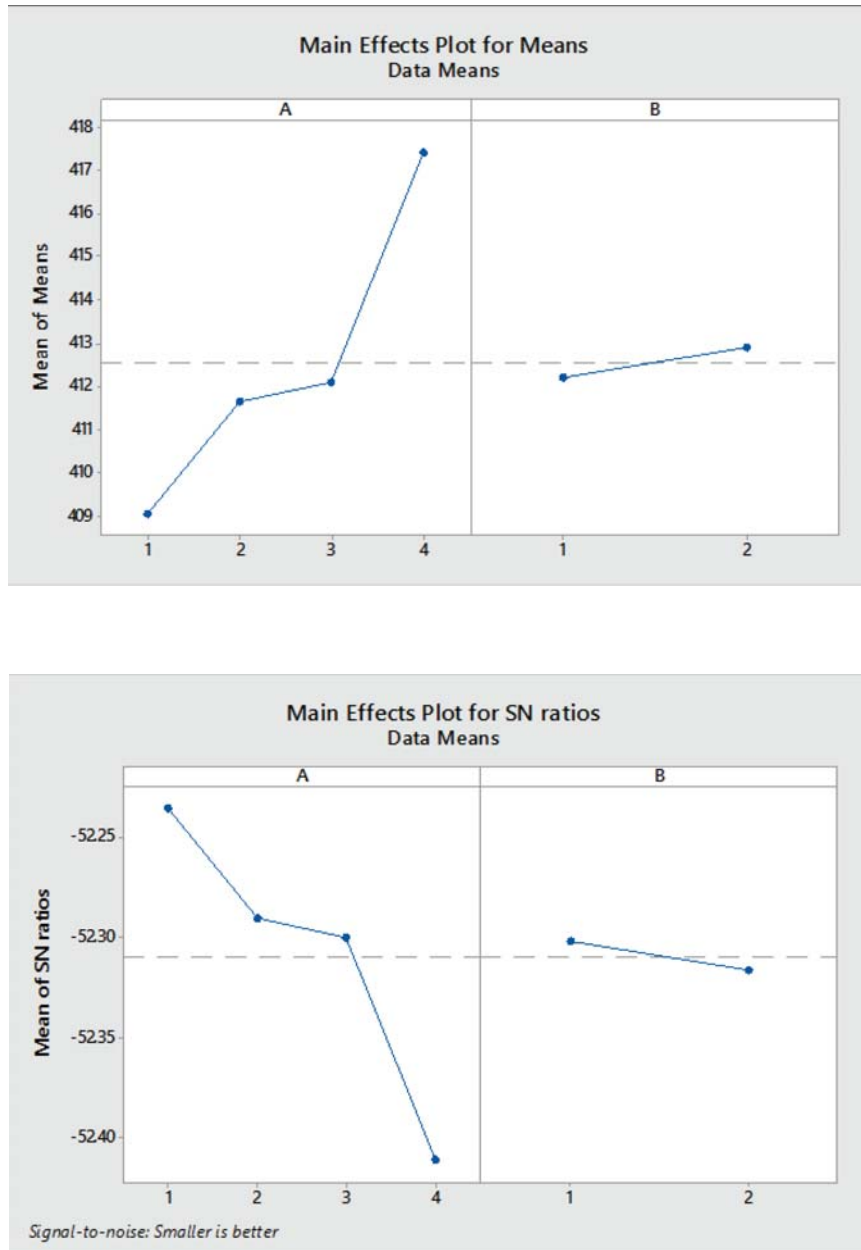




(a)



(b)



(c)

**Figure 9.** Influences of S/N and mean ratios of all parameters related to the crack defect with different angle: (a) zero; (b) 45; and (c) 90.

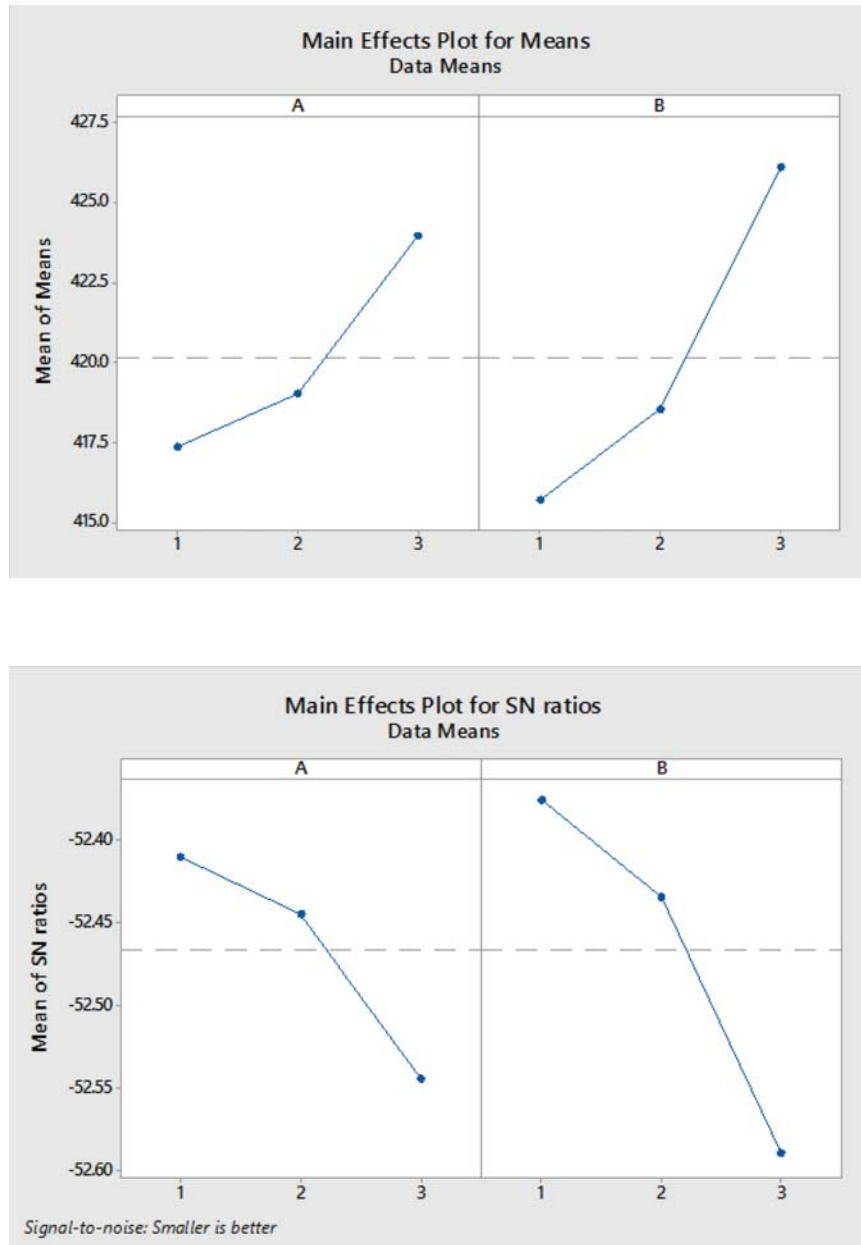


**Figure 10.** Influences of S/N and mean ratios of all parameters related to the pitting corrosion defect.

As shown in Figures 9 and 10, the run number is sufficient to perform advisement Taguchi analysis. Because, the diagram pattern of S/N ratios is reverse in compared with diagram pattern of mean ratios. On the other hand, the maximum situation in the diagram of S/N ratio is the minimum value at the diagram of the mean ratio. Next, the effect of different parameters of crack on the maximum Von Misses stress is demonstrated in Figure 11. Moreover, the impact of different parameters of pitting corrosion defect in percentage is displayed in Figure 12.

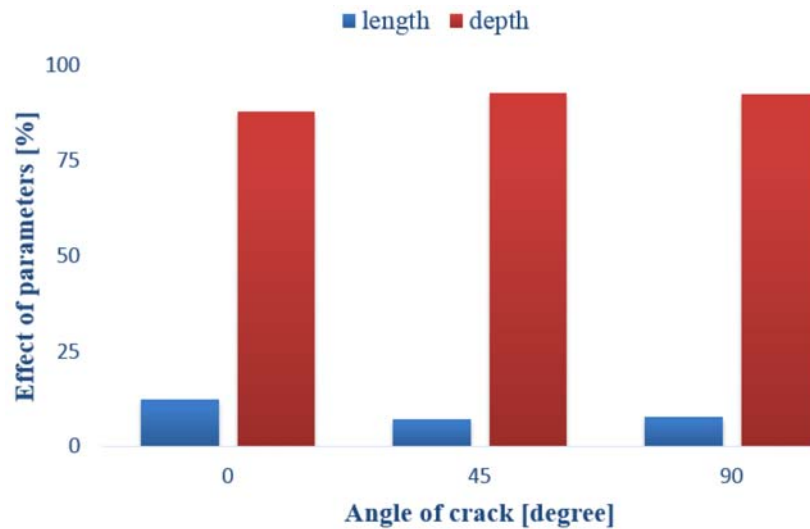


**Figure 11.** Effect of different parameters of crack with various angle.

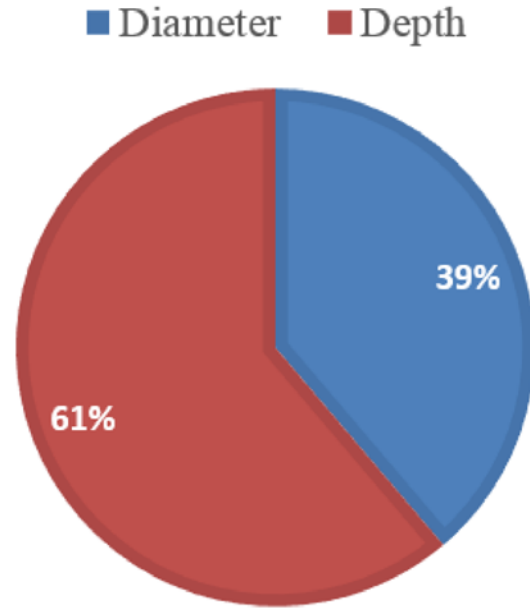


**Figure 12.** Impact of different parameters of pitting corrosion defect in percentage.

As shown in Figure 11, it is clear that the effect of crack depth increase by raising the crack angle. Also, the effect of crack length decrease by raising the angle of crack.

## 6. Conclusion

It is shown that the most critical area for crack and pitting corrosion is the second region of the tank body based on the software and analytical calculations. Although in the first region with the highest thickness of the wall, the hydrostatic pressure has a maximum value. But, the results have been shown that the second region of the oil storage tank is critical because of its supporting conditions. Also, the finite element results indicated that the most critical angle for crack is 45 degrees. Moreover, the obtained results showed that the effect of crack depth on the increasing of stress is more than the effect of crack length. And for the

defect of pitting corrosion, the impact of depth on the stress raising is more than the impact of diameter. On the other hand, the progression towards depth has a greater effect on the equivalent Von Misses stress over progression towards its length. Moreover, Taguchi analysis indicated that the effect of crack depth on the maximum Von Misses stress at the critical region of the oil storage tank is about 91% and the effect of crack length is 9%. In addition, the effect of pit depth and diameter on the critical stress at corrosion defect is about 61% and 39%, respectively.

### References

- [1] J. Underwood, Stress intensity factors for internally pressurized thick-walled cylinders, *Stress Analysis and Growth of Cracks*, ASTM STP 513 (1997), 59-70.
- [2] I. S. Raju and J. C. Newman, Stress-intensity factor for internal and external surface cracks in cylindrical vessels, *Journal of Pressure Vessel Technology* 104(4) (1982), 293-298.  
DOI: <https://doi.org/10.1115/1.3264220>
- [3] A. Carpinteri, Shape change of surface cracks in round bars under cyclic axial loading, *International Journal of Fatigue* 15(1) (1993), 21-26.  
DOI: [https://doi.org/10.1016/0142-1123\(93\)90072-X](https://doi.org/10.1016/0142-1123(93)90072-X)
- [4] A. Carpinteri, R. Brighenti and A. Spagnoli, Part-through cracks in pipes under cyclic bending, *Nuclear and Engineering Design* 185(1) (1998), 1-10.  
DOI: [https://doi.org/10.1016/S0029-5493\(98\)00189-7](https://doi.org/10.1016/S0029-5493(98)00189-7)
- [5] M. Fonte and M. Freitas, Stress intensity factors for semi-elliptical surface cracks in round bars under bending and torsion, *International Journal of Fatigue* 21(5) (1999), 457-463.  
DOI: [https://doi.org/10.1016/S0142-1123\(98\)00090-5](https://doi.org/10.1016/S0142-1123(98)00090-5)
- [6] M. Fonte, E. Gomes and M. Freitas, Stress intensity factors for semi-elliptical surface cracks in round bars subjected to mode I (bending) and mode III (torsion) loading, *Multiaxial Fatigue and Fracture*, 25 ESIS Publication (1999), 249-260.  
DOI: [https://doi.org/10.1016/S1566-1369\(99\)80019-3](https://doi.org/10.1016/S1566-1369(99)80019-3)
- [7] G. S. Bhuyan, E. J. Sperling, G. Shen, H. Yin and M. D. Rana, Prediction of failure behavior of a welded pressure vessel containing flaws during a hydrogen-charged burst test, *Journal of Pressure Vessel Technology* 121(3) (1999), 246-251.  
DOI: <https://doi.org/10.1115/1.2883699>

- [8] A. Carpinteri, R. Brighenti and A. Spagnoli, Fatigue growth simulation of part-through flaws in thick-walled pipes under rotary bending, *International Journal of Fatigue* 22(1) (2000), 1-9.  
DOI: [https://doi.org/10.1016/S0142-1123\(99\)00115-2](https://doi.org/10.1016/S0142-1123(99)00115-2)
- [9] Development of Accept Reject Criteria for Requalification of High Pressure Steel and Aluminium Cylinder, The Center of Nondestructive Testing Information Analysis, Final Report, July 2002.
- [10] A. R. Shahani and S. E. Habibi, Calculation of stress intensity factors for semi-elliptical surface cracks in thick-walled cylinders under bending moment-Part I: Numerical simulation, 14<sup>th</sup> Annual International Conference of Iranian Society of Mechanical Engineering, Isfahan University, Isfahan, 2007.
- [11] A. R. Shahani, M. Mohammadi Shoja, A. Fazli and M. Hosseinali, Calculation of stress intensity factors for semi-elliptical surface cracks in thick-walled cylinders under bending moment-Part II: Experimental observations, 14<sup>th</sup> Annual International Conference of Iranian Society of Mechanical Engineering, Isfahan University, Isfahan, 2007.
- [12] C. D. Wallbrink, D. Peng and R. Jones, Assessment of partly circumferential cracks in pipes, *International Journal of Fracture* 133(2) (2005), 167-181.  
DOI: <https://doi.org/10.1007/s10704-005-0628-0>
- [13] A. R. Shahani and S. E. Habibi, Stress intensity factors in a hallow cylinder containing a circumferential semi-elliptical crack subjected to combined loading, *International Journal of Fatigue* 29(1) (2007), 128-140.  
DOI: <https://doi.org/10.1016/j.ijfatigue.2006.01.017>
- [14] A. Kaptan and Y. Kisioglu, Determination of burst pressure and failure locations of vehicle LPG cylinders, *International Journal of Pressure Vessels and Piping* 87(4) (2007) 451-459.  
DOI: <https://doi.org/10.1016/j.ijpvp.2007.02.004>
- [15] N. Kasai, Y. Fujiwara, K. Sekine and T. Sakamoto, Evaluation of back-side flaws of the bottom plates of an oil-storage tank by the RFECT, *NDT & E International* 41(7) (2008), 525-529.  
DOI: <https://doi.org/10.1016/j.ndteint.2008.05.002>
- [16] J. S. Kim, D. H. An, S. Y. Lee and B. Y. Lee, A failure analysis of fillet joint cracking in an oil storage tank, *Journal of Loss Prevention in the Process Industries* 22(6) (2009), 845-849.  
DOI: <https://doi.org/10.1016/j.jlp.2009.08.014>
- [17] L. A. Godoy and J. C. Batista-Abreu, Buckling of fixed-roof aboveground oil storage tanks under heat induced by an external fire, *Thin-Walled Structures* 52 (2012), 90-101.  
DOI: <https://doi.org/10.1016/j.tws.2011.12.005>



- [18] L. Yang, Z. Chen, G. Cao, C. Yu and W. Guo, An analytical formula for elastic-plastic instability of large oil storage tanks, *International Journal of Pressure Vessels and Piping* 101 (2013), 72-80.  
DOI: <https://doi.org/10.1016/j.ijpvp.2012.10.006>
- [19] N. Kasai, S. Mori, K. Tamura, K. Sekine, T. Tsuchida and Y. Serizawa, Predicting maximum depth of corrosion using extreme value analysis and Bayesian inference, *International Journal of Pressure Vessels and Piping* 146 (2016), 129-134.  
DOI: <https://doi.org/10.1016/j.ijpvp.2016.08.002>
- [20] X. Cheng, W. Jing, C. Yin and C. Li, Stability parameter analysis of a composite foundation of an oil storage tank in a loess area treated with compaction piles, *Soils and Foundations* 58(2) (2018), 306-318.  
DOI: <https://doi.org/10.1016/j.sandf.2018.02.004>
- [21] H. Shigeno and D. E. Katsutomo, Okamoto corrosion of bottom plate of oil storage tank and corrosion control, Nakagawa Corrosion Protecting Company, Ltd. Japan 1960.
- [22] Alan W. Pence, Failure Avoidance in Welded Fabrication, October, 1988.
- [23] A. Higdon, E. H. Ohlsen, W. B. Stiles, J. A. Weese and W. F. Riley, *Mechanics of materials*, Fourth Edition, John Wiley and Sons, 1985.
- [24] ABAQUS Analysis User Manual, Version 6.6, Hibbit, Karlsson & Sorensen Inc., 2006.
- [25] MSC/PATRAN & MSC/NASTRAN Analysis User Manual, 2001.
- [26] X. Liu, S. Zhao, Y. Qin, J. Zhao and W. A. Wan-Nawang, A parametric study on the bending accuracy in micro W-bending using Taguchi method, *Measurement* 100 (2017), 233-242.  
DOI: <https://doi.org/10.1016/j.measurement.2016.12.007>
- [27] A. M. Hebbale and M. S. Srinath, Taguchi analysis on erosive wear behavior of cobalt based microwave cladding on stainless steel AISI-420, *Measurement* 99 (2017), 98-107.  
DOI: <https://doi.org/10.1016/j.measurement.2016.12.024>
- [28] K. Abd, K. Abhary and R. Marian, Multi-objective optimization of dynamic scheduling in robotic flexible assembly cells via fuzzy-based Taguchi approach, *Computers & Industrial Engineering* 99 (2016), 250-259.  
DOI: <https://doi.org/10.1016/j.cie.2016.07.028>
- [29] N. Pandey, K. Murugesan and H. R. Thomas, Optimization of ground heat exchangers for space heating and cooling applications using Taguchi method and utility concept, *Applied Energy* 190 (2017), 421-438.  
DOI: <https://doi.org/10.1016/j.apenergy.2016.12.154>

- [30] L. Zhao, Y. Zhao, C. Bao, Q. Hou and A. Yu, Optimisation of a circularly vibrating screen based on DEM simulation and Taguchi orthogonal experimental design, *Powder Technology* 310 (2017), 307-317.

DOI: <https://doi.org/10.1016/j.powtec.2017.01.049>

- [31] R. Chauhan, T. Singh, N. Kumar, A. Patnaik and N. Thakur, Experimental investigation and optimization of impinging jet solar thermal collector by Taguchi method, *Applied Thermal Engineering* 116 (2017), 100-109.

DOI: <https://doi.org/10.1016/j.applthermaleng.2017.01.025>

